Intrinsic Capacity of the MIMO Wireless Channel *

Jon W. Wallace and Michael A. Jensen
(wall@ieee.org) (jensen@ee.byu.edu)
Department of Electrical and Computer Engineering
459 CB, Brigham Young University, Provo, UT 84602-4099

Abstract

This paper presents a new framework for the information-theoretic analysis of multiple-input multiple-output (MIMO) wireless communications channels in the presence of multipath. This approach defines an upper bound on transmission that is independent of the antenna types and array configurations and only depends on the physical propagation scenario. Transmit sources and receive sensors are abstracted in terms of spatial basis functions. The "intrinsic capacity" of the channel is defined as the maximum mutual information of the transmit and receive vectors over all possible modulation, transmit basis functions, and receive basis functions, constrained by fixed average radiated power, limited transmit and receive volumes, and sensor noise. Definition of a "coherence matrix" allows a closed-form solution for the capacity under a new radiated power constraint.

1 Introduction

Information-theoretic analyses [3, 6] and real propagation measurements have demonstrated the capacity advantage of multiple-input multiple-output (MIMO) systems over single-antenna systems for wireless communications over multipath channels. In these prior studies, the transmit and receive arrays are generally fixed, and the "channel" is described by a finite-dimensional channel transfer matrix that relates the response of each receive antenna to the excitation of each transmit antenna. Channel capacity may then be computed with available techniques [2, 3, 6].

Interestingly, altering the type of antennas employed or the array configuration may substantially increase capacity [1, 9]. This influence of the physical antenna characteristics suggests that capacity computed for fixed arrays does not represent a true upper bound on achievable performance for a specific channel. This bound is important as, without it, no true definition of optimality for MIMO communications is possible.

We propose a new framework for computing the capacity of electromagnetic channels that is independent of the transmit and receive antenna characteristics. Given a realistic channel model and very general operational principles of the antenna elements, this framework yields capacity, referred to here as *intrinsic capacity*, that represents the maximum mutual information over *all* possible transmission system parameters (coding, signal processing, and antenna configurations). The resulting capacity therefore provides an ultimate upper bound on antenna array performance for MIMO systems and defines a point of diminishing returns for effort in physical antenna design.

2 Continuous-Space Channel Model

The model adopted here is very similar to recent work for modeling optical communication between volumes in free space [5]. Figure 1 depicts an arbitrary propagation scenario, where the transmit elements (or *sources*) and receive elements (or *sensors*) are confined to the volumes $\Delta V'$ and ΔV respectively. The channel is defined as the response of electromagnetic fields in the transmit and receive spaces to a continuous current distribution in the transmit volume.

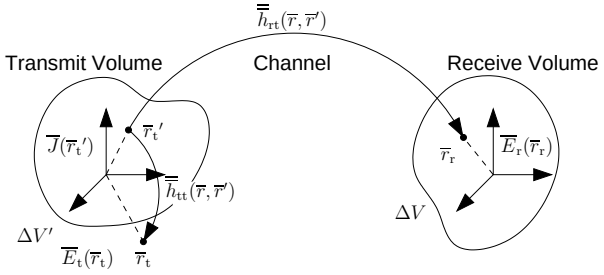

Figure 1. Intrinsic capacity channel model

*This work was supported by the National Science Foundation under Wireless Initiative Grant CCR 99-79452 and Information Technology Research Grant CCR-0081476.

From electromagnetic wave theory [4], the electric field response in the transmit and receive spaces is given by

$$\overline{E}_{\rm t}(\overline{r}_{\rm t}) = \int_{\Delta V'} d\overline{r}_{\rm t}{}' \, \overline{\overline{h}}_{\rm tt}(\overline{r}_{\rm t}, \overline{r}_{\rm t}{}')\overline{J}(\overline{r}_{\rm t}{}')$$
$$\overline{E}_{\rm r}(\overline{r}_{\rm r}) = \int_{\Delta V'} d\overline{r}_{\rm t}{}' \, \overline{\overline{h}}_{\rm rt}(\overline{r}_{\rm r}, \overline{r}_{\rm t}{}')\overline{J}(\overline{r}_{\rm t}{}'), \qquad (1)$$

where $\overline{E}_{\rm t}(\overline{r}_{\rm t})$ and $\overline{E}_{\rm r}(\overline{r}_{\rm r})$ are the vectorial electric fields in the transmit and receive spaces, respectively, $\overline{J}(\overline{r}_{\rm t}{}')$ is the vectorial current distribution confined to the transmit volume $\Delta V'$, and $\overline{\overline{h}}_{\rm tt}$ and $\overline{\overline{h}}_{\rm rt}$ are generalized dyadic Green's functions.

Since practical systems have a finite number of transmit data streams, we represent the transmit current distribution as a linear combination of modulated current source basis functions or

$$\overline{J}(\overline{r}_{\rm t}{}') = \sum_i X_i \overline{T}_i(\overline{r}_{\rm t}{}'), \qquad (2)$$

where X_i is the complex weight applied to the basis function $\overline{T}_i$. Similarly, the sensors compute the generalized voltage measurement

$$Y_k = \int_{\Delta V} d\overline{r}_{\rm r} \, \overline{R}_k^H(\overline{r}_{\rm r})\overline{E}_{\rm r}(\overline{r}_{\rm r}) + N_k, \qquad (3)$$

where $\{\cdot\}^H$ is the Hermitian operator, Y_k is the voltage measurement of the kth sensor employing the receive basis function $\overline{R}_k$, and N_k is measurement noise or error. To avoid arbitrary scaling of the channel response, source power is limited by the radiated power constraint in Section 3, and the receive basis functions are constrained to be orthonormal. Substitution of (1) and (2) into (3) yields the matrix equation

$$\overline{Y} = \overline{\overline{H}} \, \overline{X} + \overline{N}, \qquad (4)$$

where the discrete response matrix elements are given as

$$H_{ki} = \int_{\Delta V} d\overline{r}_{\rm r} \int_{\Delta V'} d\overline{r}_{\rm t}{}' \, \overline{R}_k^H(\overline{r}_{\rm r})\overline{\overline{h}}_{\rm rt}(\overline{r}_{\rm r}, \overline{r}_{\rm t}{}')\overline{T}_i(\overline{r}_{\rm t}{}'). \qquad (5)$$

Thus, for fixed transmit and receive basis functions, the capacity of the channel represented by $\overline{\overline{H}}$ may be computed using standard techniques [2, 3, 6]. In order for this capacity to represent the intrinsic capacity of the channel, however, an optimal set of basis functions must be determined. In this context, the intrinsic capacity is defined as the maximum mutual information of the vectors $\overline{Y}$ and $\overline{X}$ over all possible source functions ($\overline{R}$), sensor functions ($\overline{T}$), and modulation ($\overline{X}$), with the sources and sensors confined to their respective volumes.

For arbitrary Green's functions and arbitrary source and sensor volume shapes, no simple procedure for finding the optimal basis functions appears to exist. However, close approximations to the continuous-space sensor functions may be obtained with the following numerical method. We define sub-basis functions that span the transmit and receive spaces in a limiting sense as the number of sub-basis functions becomes infinite. The transmit and receive basis functions are then written as a linear combination of the sub-basis functions or,

$$\overline{T}_i(\overline{r}') = \sum_n c_{ni}\overline{\mathcal{T}}_n(\overline{r}') \qquad \overline{R}_k(\overline{r}) = \sum_n b_{nk}\overline{\mathcal{R}}_n(\overline{r}). \quad (6)$$

If these sub-basis functions are orthonormal, then substitution of these expressions into (3) results in

$$H_{ki} = \int_{\Delta V} d\overline{r}_{\rm r} \int_{\Delta V'} d\overline{r}_{\rm t}{}' \left[\sum_m b_{mk}\overline{\mathcal{R}}_m(\overline{r}_{\rm r})\right]^H \times \overline{\overline{h}}_{\rm rt}(\overline{r}_{\rm r}, \overline{r}_{\rm t}{}') \sum_n c_{ni}\overline{\mathcal{T}}_n(\overline{r}_{\rm t}{}')$$
$$= \sum_m \sum_n b_{mk}^* \mathcal{H}_{mn} c_{ni}. \qquad (7)$$

Representing the matrix $\overline{\overline{\mathcal{H}}}$ in terms of its singular value decomposition (SVD) $\overline{\overline{\mathcal{H}}} = \overline{\overline{\mathcal{U}}} \, \overline{\overline{\mathcal{S}}} \, \overline{\overline{\mathcal{V}}}^H$ and performing the assignments $c_{ni} = \mathcal{V}_{ni}$ and $b_{km} = \mathcal{U}_{km}$ yields $H_{ki} = \delta_{ki}\mathcal{S}_{kk}$. Also, since the sub-basis functions are constrained to be orthonormal, this assignment ensures that the transmit and receive basis functions are also orthonormal. In this case, the expression for mutual information of the vectors $\overline{Y}$ and $\overline{X}$ becomes

$$I(\overline{Y}, \overline{X}) \le \log_2 \left| \frac{\overline{\overline{\mathcal{S}}} \, \overline{\overline{k}}_x \, \overline{\overline{\mathcal{S}}}}{\sigma^2} + \overline{\overline{I}} \right|, \qquad (8)$$

where $\overline{\overline{k}}_x$ is the transmit covariance matrix, σ^2 is the single receiver noise variance, and equality is attained for complex Gaussian signaling. If $\overline{\overline{k}}_x$ is chosen to maximize (8) and the number of sub-basis functions becomes large, (8) converges to the intrinsic capacity bound.

The analysis of a full vectorial three-dimensional scenario is very complicated and tends to obscure the basic technique. In this paper we assume a very simple single-polarization two-dimensional path-based channel model with

$$\overline{\overline{h}}_{\rm rt}(\overline{r}, \overline{r}') = \overline{\overline{I}} \sum_\ell \beta_\ell \, \exp[jk_0(x\cos\theta_{{\rm r}\ell} + y\sin\theta_{{\rm r}\ell})] \times \exp[jk_0(x'\cos\theta_{{\rm t}\ell} + y'\sin\theta_{{\rm t}\ell}), \qquad (9)$$

where $\overline{k}'$ and $\overline{k}$ are the source and receive wavenumbers, respectively, β_ℓ is the complex gain of the ℓth ray, and $\theta_{{\rm r}\ell}$ and $\theta_{{\rm t}\ell}$ are the arrival and departure angles of the ℓth ray. Also, $\overline{\overline{h}}_{\rm tt}(\overline{r}, \overline{r}')$ is assumed to be the standard three-dimensional free-space Green's function [4].

3 Radiated Power Constraint

Previous analyses of MIMO systems generally assume a simple trace constraint on the transmit element covariance, ignoring possible coherent coupling effects at the transmitter. Since our intrinsic capacity framework employs many closely spaced elements with possibly high coupling, we develop a new constraint that limits the expected radiated transmit power of the system. For an ergodic transmit distribution, this limit is closely related to the Effective Isotropic Radiated Power (EIRP) constraint imposed on many real-world communications systems.

In many physical problems, instantaneous radiated power is related to the complex transmit element voltages or currents according to the relation

$$P_{\mathrm{rad}} = \overline{X}^H \overline{\overline{A}}\, \overline{X}, \tag{10}$$

where $\overline{\overline{A}}$ is a Hermitian *coherence matrix* and $\overline{X}$ is the vector of transmit element voltages or currents. When this relation holds, the average radiated power is given as

$$\mathrm{E}\{P_{\mathrm{rad}}\} = \mathrm{E}\left\{\overline{X}^H \overline{\overline{A}}\, \overline{X}\right\} = \mathrm{Tr}(\overline{\overline{k}}_x\, \overline{\overline{A}}). \tag{11}$$

The capacity of an N_R receive by N_T transmit MIMO wireless system becomes

$$\max_{\overline{\overline{k}}_x} \log_2 \left| \frac{\overline{\overline{H}}\, \overline{\overline{k}}_x\, \overline{\overline{H}}^H}{\sigma^2} + \overline{\overline{I}} \right| \tag{12}$$

subject to $\mathrm{Tr}(\overline{\overline{k}}_x\, \overline{\overline{A}}) = P_T$, where $\overline{\overline{H}}$ is the $N_R \times N_T$ channel matrix, σ^2 is the single receive element sensor noise variance, $\overline{\overline{k}}_x$ is the transmit covariance, and P_T is the allowed total average transmit power. When $\overline{\overline{H}}$ has poor numerical conditioning, care is required to evaluate this maximum. In this case, (12) is rewritten as

$$\max_{\overline{\overline{k}}_x^S} \log_2 \left| \frac{\overline{\overline{S}}\, \overline{\overline{k}}_x^S\, \overline{\overline{S}}}{\sigma^2} + \overline{\overline{I}} \right| \tag{13}$$

where $\overline{\overline{S}}$ is a diagonal matrix containing the N_S most significant singular values of $\overline{\overline{H}}$, $\overline{\overline{k}}_x^S = \overline{\overline{V}}\, \overline{\overline{k}}_x\, \overline{\overline{V}}^H$ is a new transmit covariance, and $\overline{\overline{V}}$ is the matrix of right singular vectors of $\overline{\overline{H}}$. The number of singular values may be limited by imposing a maximum allowed conditioning number on $\overline{\overline{S}}$.

Next, we apply the substitution

$$\overline{\overline{k}}_x^S = \overline{\overline{S}}^{-1} \overline{\overline{\xi}}_Z \overline{\overline{\Lambda}}_Z^{1/2} \overline{\overline{k}}_x^Z \overline{\overline{\Lambda}}_Z^{1/2} \overline{\overline{\xi}}_Z^H \overline{\overline{S}}^{-1}, \tag{14}$$

where we have performed the eigenvalue decomposition (EVD) of $\overline{\overline{S}}\, \overline{\overline{A}}_S^{-1} \overline{\overline{S}} = \overline{\overline{\xi}}_Z \overline{\overline{\Lambda}}_Z \overline{\overline{\xi}}_Z^H$, which transforms the mutual information expression in (13) to

$$I(\overline{Y}; \overline{X}) = \log_2 \left| \frac{\overline{\overline{\Lambda}}_Z^{1/2} \overline{\overline{k}}_x^Z \overline{\overline{\Lambda}}_Z^{1/2}}{\sigma_N^2} + \overline{\overline{I}} \right| \tag{15}$$

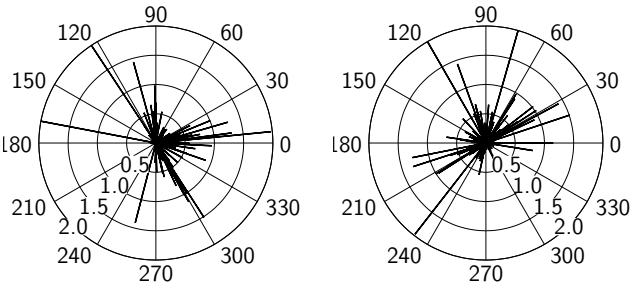

(a) Transmit (b) Receive

Figure 2. Transmit and receive rays

r	C_{std}	C_{prad}	P_{std}	P_{prad}
0.125 λ	25.1	29.5	2.504	1.000
0.250 λ	31.5	34.9	1.367	1.000
0.500 λ	38.1	38.8	0.950	1.000
1.000 λ	39.5	40.3	0.993	1.000
2.000 λ	41.3	42.1	1.021	1.000
4.000 λ	42.2	42.4	1.043	1.000
8.000 λ	43.1	43.2	1.017	1.000

Table 1. Capacity and radiated power for circular arrays

and the power constraint to simply $\mathrm{Tr}(\overline{\overline{k}}_x^Z) = P_T$. This problem is now appropriate for the water-filling solution.

A single numerical example demonstrates differences between the new radiated power constraint and the standard trace power constraint. Consider eight-element uniform circular arrays at transmit and receive with array radii of r. The two dimensional path-based ray model in (9) is assumed with the departure and arrival directions and gains depicted in Figure 2. The length and direction of each impulse in the plot correspond to the amplitude and the angle-of-arrival/departure of each ray, respectively. These rays were generated with a single random realization of the Saleh-Valenzuela Angular (SVA) model [7, 8, 10] with parameters $\Gamma = 1$, $\Lambda = 2$, $\gamma = 1$, $\lambda = 6$, $\sigma = 26^\circ$.

Table 1 lists the capacity (C) and average radiated power (P) for the standard trace power constraint (std) and for the new radiated power constraint (prad) versus array radii. In each case, noise power was fixed to obtain a single-input single-output (SISO) signal-to-noise ratio (SNR) of 20 dB. Total power was $P_T = 1$, and power radiated was calculated assuming a coherence matrix appropriate for superimposed Hertzian dipoles. For close spacings, $\mathrm{Tr}(\overline{\overline{k}}_x \overline{\overline{A}})$ may be substantially larger than $\mathrm{Tr}(\overline{\overline{k}}_x)$ due to the coherent interaction

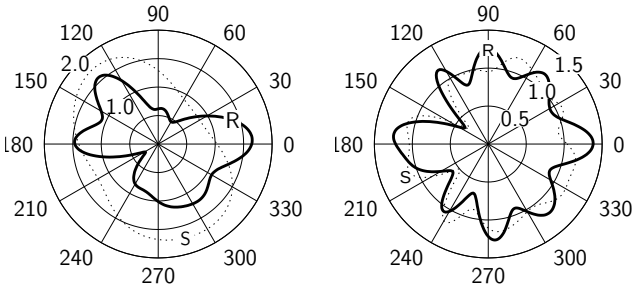

(a) $r = 0.25\lambda$ (b) $r = 1.0\lambda$

Figure 3. Average radiated power

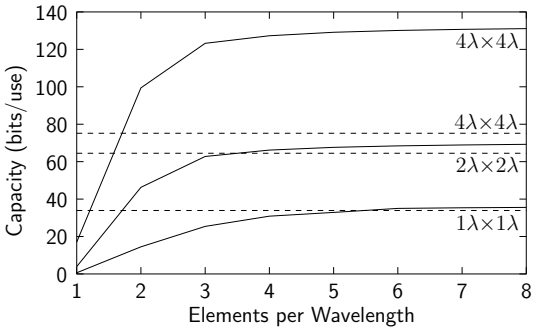

Figure 4. Site-specific intrinsic capacity

of radiated fields. However, for larger spacings, the radiated power converges to the expected value of 1. Surprisingly, the capacity obtained with the radiated power constraint is higher than that obtained with the standard trace power constraint, suggesting the exploitation of transmit directions that have high signal transfer with modest overall radiated power. However, other examples may be constructed where the opposite is true. Figure 3 depicts the average transmit power density as a function of angle for the $r = 0.25\lambda$ and $r = 1.0\lambda$ cases for the standard constraint (S) and the radiated power constraint (R). For close spacings, the patterns are quite different and the radiated power constraint favors a more directive pattern. For large spacing, the patterns become nearly identical.

4 Intrinsic Capacity Computations

In this section, we apply the intrinsic capacity framework from Section 2 with the radiated power constraint in Section 3 to compute the intrinsic capacity of hypothetical propagation scenarios.

Square boxes were assumed for the transmit and receive volumes having dimensions Δx, $\Delta y = \Delta x$, and Δz. Estimates of the intrinsic capacity were obtained by applying the approximate numerical method in Section 2. Box-shaped sub-basis functions of the form

$$\begin{matrix}\mathcal{R}_i(\overline{r}) \\ \mathcal{T}_i(\overline{r})\end{matrix} = \begin{cases} \frac{N}{\sqrt{\Delta x \Delta y \Delta z}}, & \begin{matrix} x_i - \frac{\Delta x}{2N} < x < x_i + \frac{\Delta x}{2N} \\ y_i - \frac{\Delta y}{2N} < y < y_i + \frac{\Delta y}{2N} \\ -\frac{\Delta z}{2} < z < \frac{\Delta z}{2} \end{matrix} \\ 0, & \text{otherwise,} \end{cases} \tag{16}$$

were assumed, where N is the number of subdivisions in x and y, and (x_i, y_i) defines the center of the support region for the ith basis function. For comparison, capacity was also computed for a 16-element dipole array with elements placed near the surface of the antenna volumes. A fair comparison is obtained by letting $\Delta z = \lambda/2$ and limiting the gain of the dipoles so that power collected by the dipole array cannot exceed the power collected by sub-basis functions spanning the complete receive volume. This limitation is realistic since only a finite amount of power is incident on the receive volume. In each case, the noise power is fixed by assuming a single dipole at transmit and receive and adjusting the noise to obtain an average SNR of 20 dB for a single antenna system.

4.1 Site-Specific Intrinsic Capacity

This section presents capacity computations for a single channel with the ray structure at transmit and receive depicted in Figure 2. Figure 4 plots the intrinsic capacity estimates given by the box-shaped sub-basis as a function of the number of sub-basis sources/sensors per wavelength (solid lines) and the capacity of the 16-element dipole array (dashed lines) for comparison. Results for three different allowed antenna areas ($\Delta x \times \Delta y$) are depicted: $1\lambda \times 1\lambda$, $2\lambda \times 2\lambda$, and $4\lambda \times 4\lambda$. Two important features of intrinsic capacity are apparent in the plot. First, the capacity of the box-shaped sensors approaches a horizontal asymptote (the intrinsic capacity) as the sampling resolution increases. A good estimate of the intrinsic capacity is reached for about 6 elements per wavelength. Second, for small antenna area, the 16-element dipole array nearly achieves the intrinsic capacity limit. However, for larger areas, the discrepancy widens. The difference is due to two main limitations of the dipole array: (1) for large areas the fields are undersampled, and (2) the power collection capability for a fixed number of dipoles is inherently limited.

4.2 Intrinsic Capacity Statistics

Combining many realizations of the SVA model with the Monte Carlo technique provides insight into the statistical behavior of the intrinsic capacity. Here, box-shaped

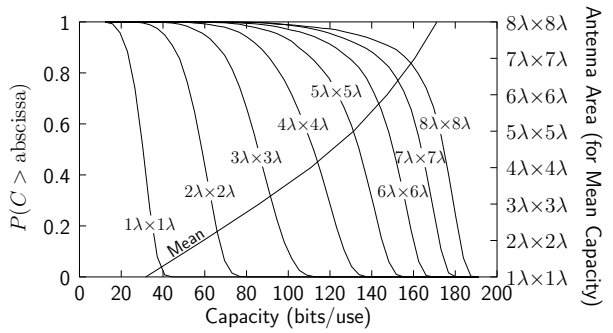

Figure 5. Intrinsic capacity vs. area

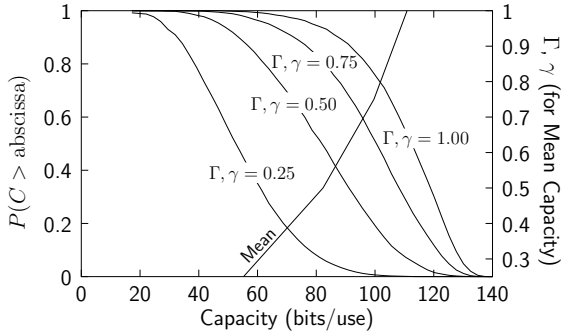

Figure 6. Intrinsic capacity vs. multipath

sensors with a sampling resolution of 8 sensors per wavelength provide close estimates of the intrinsic capacity. The SVA model parameters controlling multipath delay and angle spread as well as the number of multipath arrivals were $\Gamma = 1$, $\Lambda = 2$, $\gamma = 1$, $\lambda = 6$, $\sigma = 26^\circ$. 5000 channel realizations were generated to approximate each probability distribution.

Figure 5 depicts complimentary cumulative distribution functions (CCDFs) of intrinsic capacity and mean intrinsic capacity versus the allowed antenna area ($\Delta x \Delta y$). Since the SVA model parameters were fixed in these simulations, the available multipath was also fixed. For a small antenna area, the capacity increases almost linearly with the allowed antenna dimensions. As the antenna dimensions increase, however, the intrinsic capacity approaches an upper bound.

Figure 6 plots CCDFs of intrinsic capacity and mean intrinsic capacity versus the SVA multipath parameters Γ and γ, with larger values of Γ and γ corresponding to more available multipath. In this study, the constant SVA model parameters and the receiver noise were equivalent to those in the previous study. The antenna area was fixed at $4\lambda\times4\lambda$ with 8 box-shaped elements per wavelength. As before, 5000 realizations were performed to estimate each probability distribution. This study demonstrates that antenna aperture strongly limits the intrinsic capacity, even when the available multipath grows large.

5 Conclusion

This paper has presented a new framework for analysis of the continuous-space electromagnetic channel, defining an ultimate upper bound on the available capacity for constrained antenna volumes, radiated power, and receiver noise. We have defined this capacity bound as "intrinsic capacity" since it represents a capacity limitation of the physical propagation environment that is independent of the system-specific antennas and array geometries. Representative simulations compared the intrinsic capacity bound with a physically realizable array and demonstrated the statistical behavior as a function of the allowed antenna volume and available multipath.

References

[1] R. A. Andrews, P. P. Mitra, and R. deCarvalho. Tripling the capacity of wireless communications using electromagnetic polarization. *Nature*, 409:316–318, Jan. 2001.

[2] T. M. Cover and J. A. Thomas. *Elements of Information Theory*. John Wiley & Sons, 1991.

[3] G. J. Foschini and M. J. Gans. On limits of wireless communications in a fading environment when using multiple antennas. *Wireless Personal Communications*, 6:311–335, Mar. 1998.

[4] J. A. Kong. *Electromagnetic Wave Theory*. John Wiley & Sons, 1990.

[5] D. A. Miller. Communicating with waves between volumes: evaluating orthogonal spatial channels and limits on coupling strengths. *Applied Optics*, 39:1681–1699, Apr. 2000.

[6] G. G. Raleigh and J. M. Cioffi. Spatio-temporal coding for wireless communication. *IEEE Transactions on Communications*, 46:357–366, Mar. 1998.

[7] A. A. M. Saleh and R. A. Valenzuela. A statistical model for indoor multipath propagation. *IEEE Journal on Selected Areas in Communications*, SAC-5:128–137, Feb. 1987.

[8] Q. H. Spencer, B. D. Jeffs, M. A. Jensen, and A. L. Swindlehurst. Modeling the statistical time and angle of arrival characteristics of an indoor multipath channel. *IEEE Journal on Selected Areas in Communications*, 18:347–360, Mar. 2000.

[9] J. W. Wallace and M. A. Jensen. Characteristics of measured 4x4 and 10x10 MIMO wireless channel data at 2.4-GHz. In *IEEE AP-S 2001*, volume 3, pages 96–99, Boston, MA, July 8-13 2001.

[10] J. W. Wallace and M. A. Jensen. Statistical characteristics of measured MIMO wireless channel data and comparison to conventional models. In *IEEE VTC'2001 Fall Conf.*, volume 2, pages 1078–1082, Atlantic City, NJ, Oct. 7-11 2001.